Stimulated microwave emission from E×B drifting electrons in slow-wave cavities: A quantum approach

Spilios Riyopoulos
Science Application International Corporation, McLean, Virginia 22102
(Received 17 August 1994)

Stimulated microwave emission from **E×B** drifting electrons in slow-wave cavities occurs when the Doppler-shifted radiation frequency is either near zero or the electron cyclotron frequency. The former case, characterized by the synchronous drift velocity u, $\omega - ku \simeq 0$, corresponds to the "pure drift" instability, while the latter, satisfying $\omega - ku \simeq \pm\Omega$, is termed the "drift-cyclotron" mode. In both cases the drift kinetic energy and momentum are invariant during radiative transitions. The momentum of the emitted or absorbed radiation quantum comes from the vector potential associated with the static magnetic field and induces a shift of the electron guiding center in a direction transverse to the drift velocity. In the pure drift case the radiation energy comes from the change in the electrostatic potential energy. In the drift-cyclotron case both electrostatic and cyclotron rotation energies are converted into radiation. In the nonrelativistic regime the gain is symmetric with respect to the frequency detuning from resonance. The difference between the stimulated absorption and emission probabilities, responsible for the gain, is caused by field gradients across the direction of the electron drift. These gradients come from the waveguide mode structure and the collective field of the electron beam. The drift mode is always unstable, while there exists one stable and one unstable drift-cyclotron branch. Relativistic mass effects influence only the drift-cyclotron instability, adding a gain contribution that is antisymmetric in frequency detuning.

PACS number(s): 52.75.Ms, 85.10.Jz, 42.52.+x, 42.55.−f

I. INTRODUCTION

The stimulated microwave emission from electrons undergoing **E×B** drift in crossed electric and magnetic fields is the physical principle underlying the operation of magnetrons [1,2] and crossed-field amplifiers [3] (CFA's), the earliest developed sources for coherent microwave generation. Magnetrons and CFA's fall into a general class of devices, including the electron cyclotron masers [4] (ECM's), the free electron lasers [5] (FEL's), the traveling-wave tubes, and their variations, operating by stimulated emission from unbound electrons. The term *unbound electron devices* (UED's) is coined here to distinguish all the above from lasers and masers that are powered by stimulated emission from electrons bound in atomic or molecular orbitals, as well as to emphasize that there can be no stimulated emission from electrons that are free from external fields. Recall that a free electron can only scatter a photon, but it cannot emit one since it would violate energy-momentum conservation [6].

An important distinction in the frequency response was soon realized among UED's. The observed gain vs frequency curve is *symmetric* relative to the resonant frequency for the crossed-field devices [7,8], while it is *antisymmetric* for all the rest. That behavior led to their classification as *M*- and *O*-type devices, respectively. Recent studies [9] and experiments [10] on the sheet beam CFA showed that the symmetry in the gain vs frequency curve is preserved in the nonlinear region. The classic interpretation of this behavior [9] invokes the symmetry characterizing the guiding center (GC) orbits in crossed-field devices: the GC phase space is mirror symmetric relative to opposite detunings $\pm|\Delta\omega|$. Nevertheless, a thorough understanding of the differences between *M*- and *O*-type devices lies in the fundamental process of photon emission and absorption and requires the quantum treatment of the cross-field devices.

As in all situations involving lasing, microwave amplification requires that at any instant there are more radiation quanta being emitted than absorbed. One can draw some additional differences here, first among conventional lasers and UED's in general and then among crossed-field devices and the rest of the UED's. In a conventional laser the energy levels for bound electrons are

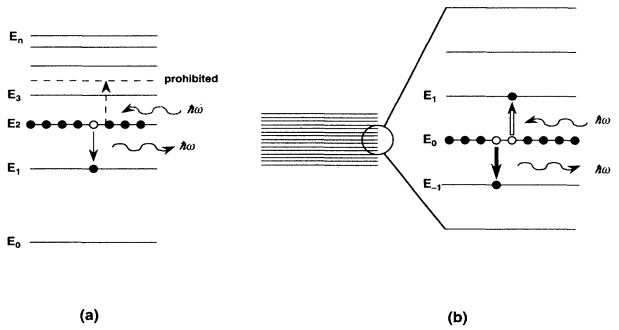

FIG. 1. Energy level spacing between (a) discrete bound electron eigenstates and (b) an unbound electron, semicontinuoum spectrum. An "inverted population" situation, where only one energy state is occupied, does not necessarily lead to radiation amplification in case (b).

unevenly spaced and a photon of given frequency can mediate transitions between only two given levels $E_2-E_1=\hbar\omega$ (excluding degeneracy), as shown in Fig. 1(a). Since the per-photon probabilities for stimulated emission and absorption are the same and since an electron at the higher energy state can only fall into the lower by emitting photons $\hbar\omega$, radiation amplification occurs simply when the number of electrons in the higher energy level exceeds that in the lower energy level. This is known as population inversion. The gain is proportional to the transition probability, thus the frequency response is *symmetric* with maximum at the exact resonance.

On the other hand, the energy spectrum for unbound electrons is typically a semicontinuous of equal energy spacing, shown in Fig. 1(b). A given frequency photon can in general induce transitions from a given energy level E_0 to either of the symmetric energy levels $E_{\pm1}=E_0\pm\hbar\omega$ above and below E_0. Since there is equal probability for stimulated transition into the lower or the higher energy state by photon emission or absorption, respectively, it appears that no amplification would occur even in case of 100% "population inversion" corresponding to a monoenergetic electron cloud and that the radiation would remain at the spontaneous emission level. The differentiation between the emission and absorption probabilities, which is necessary for net radiation gain, is introduced by the electron recoil in FEL's and the relativistic energy dependence of the cyclotron frequency in ECM's. Because of the recoil, a given energy and momentum electron in a FEL absorbs a frequency ω_a that is slightly different than the emitted frequency ω_e by the same electron, $\omega_a-\omega_e=\delta\omega$. Not surprisingly the radiation gain is proportional to the frequency *derivative* of the stimulated emission probability times $\delta\omega$, yielding the antisymmetric gain curve [11].

In a crossed-field device, operating in the slow-wave regime, the emitted photon energy stems from the electron's *electrostatic potential* energy. The emitted photon momentum comes from the electron's canonical momentum associated with the *vector potential* of the magnetic field. The drift kinetic energy and momentum remain invariant during the emission; instead of electron recoil, a parallel displacement of the electron orbit occurs. That is an essential departure compared to the rest of the UED's where the electron exchanges *kinetic energy,* and *kinematic momentum* (FEL) or *angular momentum* (ECM), with the emitted photons. It is shown that the "recoilless" emission from the **E×B** drifting electrons accounts for all the observed differences between *M*- and *O*-type devices on a fundamental level. The necessary difference between the stimulated emission and absorption probabilities is provided by electric field gradients. Gradients exist in the rf amplitude due to waveguide mode structure and are also produced by the charge distribution of the drifting electrons.

There exist two modes of interaction (dispersion branches) in a slow-wave cavity. In the "pure drift" instability $\omega-ku\simeq0$ cyclotron emission is inhibited, the cyclotron rotation quantum number being frozen during the radiative transition. The radiation gain is proportional to the transverse shift in the GC location times the spatial derivative of the overlapping integral between the initial and the final states. Since emission and absorption peak around the same frequency, the gain curve is symmetric in detuning. Net gain results from field gradients, causing a stronger overlapping between initial and final states during emission. Finite Larmor radius effects do not enter directly the energy balance during the emission or absorption of a radiation quantum. They manifest indirectly through the collective space charge effects that influence the local field gradients and thus the balance between emission and absorption rates. The gain curve of the drift instability is invariant under relativistic effects because the GC displacement is independent of γ and cyclotron transitions are prohibited.

In the drift-cyclotron branches $\omega-ku\simeq\pm|\Omega|$ the energy of the emitted quantum comes from both the electrostatic and the cyclotron oscillation energy of the electron. The drift kinetic energy and momentum are still invariants of the motion, inducing again a GC shift perpendicular to the drift direction. There is a distinction in the stability properties between the fast cyclotron branch $\omega-ku\simeq|\Omega|$ and its slow counterpart $\omega-ku\simeq-|\Omega|$. In the nonrelativistic regime the fast drift-cyclotron branch is stable due to the negative effect of the cyclotron transitions to the net emission probability. The nonrelativistic gain curve remains symmetric in detuning. Relativistic effects enter via the dependence of the cyclotron frequency on energy. The spacing between the cyclotron energy levels becomes uneven, meaning that the stimulated emission and absorption probabilities peak at different radiation frequencies. The relativistic correction to the gain, proportional to the frequency derivative of the transition probabilities, is thus antisymmetric in frequency and destabilizing for $\Omega_n>\omega-ku$. The slow drift-cyclotron branch demonstrates the opposite stability properties from the fast one.

It is worth noting that "pure cyclotron" emission at $\omega=\Omega$, characterized by a null shift in the GC location and no change in the electron potential energy, is prohibited by momentum conservation. Since the expectation value for the cyclotron oscillation momentum is zero in all states and since the drift velocity $u=cE_0/B_0$ is invariant, the change in the electron momentum required to balance the momentum of the emitted or absorbed radiation can only come from the vector potential $eA_y/c=m\Omega X$. The transverse shift of the guiding center X is thus the trademark of emission by **E×B** drifting electrons under all circumstances.

The remainder of this paper is organized as follows. Section II introduces the quantum eigenstates of the unperturbed **E×B** motion combined with cyclotron gyration. It then goes on to compute the interaction with a slow wave in the "pure drift" resonance. In Sec. III the formalism expands to include the effects of the collective electron field into the discussion. Only the laminar beam field is included; the effects of the charge perturbations on the cavity mode structure are neglected in the low gain regime. Section IV elaborates and discusses the results of Secs. II and III. The "drift-cyclotron" interaction is taken up in Sec. V by allowing transition with cyclotron emission. The nonrelativistic case is analyzed first and

the relativistic corrections are imposed by perturbative expansion. The general results and conclusions are summarized in Sec. VI.

II. STIMULATED EMISSION FROM A SYNCHRONOUS BEAM

In this section we consider the interaction between $\mathbf{E}\times\mathbf{B}$ drifting electrons and the waveguide modes in the synchronous beam case $\omega-ku\simeq 0$. The unperturbed eigenmodes for drifting electrons are derived first from Schrödinger's equation. The interaction with the rf fields is then turned on, inducing transitions between those eigenstates. The stimulated emission and absorption probabilities are finally obtained via time-dependent perturbation theory. Mutual interaction among electrons (space charge field) is for the moment ignored.

Consider a single electron moving in uniform static electric $E_0\hat{\mathbf{x}}=-\nabla\mathcal{V}_0$ and magnetic $B_0\hat{\mathbf{z}}=\nabla\times\mathbf{A}$ fields (Fig. 2). Taking $\mathcal{V}_0=-eE_0x$ and $\mathbf{A}=B_0x\hat{\mathbf{y}}$ with the canonical momentum $\mathbf{P}=-i\hbar\nabla=\mathbf{p}+(e/c)\mathbf{A}$, the nonrelativistic Schrödinger's equation is

$$i\hbar\frac{\partial\psi}{\partial t}=\mathcal{E}\psi=\mathcal{H}_0\psi=\left[-\frac{\hbar^2}{2m}\nabla^2+i\hbar\Omega x\frac{\partial}{\partial y}+\frac{1}{2}m\Omega^2x^2-eE_0x\right]\psi\ , \tag{1}$$

where $\mathcal{E}$ is the energy and $\Omega=eB_0/mc$ is the electron cyclotron frequency. Since (1) is invariant along the drift direction y, $\mathcal{H}_0$ commutes with the canonical momentum operator $\mathcal{P}_y$; hence $\mathcal{P}_y\psi=\hbar q\psi$ and $\psi(x,y)=e^{iqy}\phi(x)$. Substituting ψ inside (1) and defining

$$u=\hat{\mathbf{y}}\cdot(\mathbf{E}_0\times\mathbf{B}_0)/B_0^2=-eE_0/m\Omega \tag{2}$$

as the drift velocity gives

$$i\hbar\frac{\partial\phi_n}{\partial t}=\mathcal{E}_n\phi_n=\left[-\frac{\hbar^2}{2m}\frac{d^2}{dx^2}+\frac{1}{2}m\Omega^2(x-X_q)^2\right]\phi_n\ , \tag{3}$$

where $\mathcal{E}_n=\mathcal{E}+\frac{1}{2}mu^2-\hbar qu$ and $X_q=(\hbar q-mu)/m\Omega$ is the guiding center location. The harmonic oscillator equation (3) with energy spectrum $\mathcal{E}_n=(n+\frac{1}{2})\hbar|\Omega|$ is the quantum description of the cyclotron rotation about a GC drifting along y. Thus, if $|n,q\rangle$ symbolizes a drifting electron eigenstate with quantum numbers n and q, its wave function is

$$\psi_{n,q}(x,y;t)\equiv\langle n,q|\mathbf{x}\rangle=\phi_n(x-X_q)e^{iqy}e^{-i\mathcal{E}_nt/\hbar}\ , \tag{4}$$

where ϕ_n is given in terms of Hermite functions $\phi_n(x)=\alpha^{-1/4}\exp(-x^2/\alpha)H_n(x/\sqrt{\alpha})$ and $\alpha=\sqrt{\hbar/2m|\Omega|}$. The conserved momentum $P_y=\hbar q$ is the sum of the GC kinematic and the vector potential momentum

$$P_y=\hbar q=mu+m\Omega X_q \tag{5}$$

following the definition Eq. (3) of the GC location. Note that X_q uniquely defines the momentum and vice versa, henceforth dropping the subscript q. The total energy is

$$\mathcal{E}_{n,q}=(n+\tfrac{1}{2})\hbar|\Omega|+\hbar qu-\tfrac{1}{2}mu^2=(n+\tfrac{1}{2})\hbar|\Omega|+\tfrac{1}{2}mu^2-eE_0X\ . \tag{6}$$

The first term on the right-hand side of (6) relates to the Larmor radius via $(n+\frac{1}{2})\hbar|\Omega|=\frac{1}{2}m\Omega^2\langle\rho_n^2\rangle$, while $\frac{1}{2}mu^2-eE_0X$ are, respectively, the kinetic and the potential energies of the GC motion.

We now describe the interaction of the unbound electron eigenstates with the cavity radiation field. Adopting the old quantum treatment, the cavity modes are given by the classical solutions of Maxwell equations. For slow wave cavities $v/c\ll 1$, where v is the phase velocity, the radiation is sufficiently approximated by the ac potential

$$\mathcal{V}_1(x,y,t)=\tfrac{1}{2}V_1\sinh(kx)e^{i(ky-\omega t)} \tag{7}$$

and the interaction Hamiltonian is

$$\mathcal{H}_1=e\mathcal{V}_1(x,y,t)\ . \tag{8}$$

The per unit time transition probability between $|n,q\rangle\rightarrow|n',q'\rangle$ is expressed by the well known Fermi rule

$$\frac{dp}{dt}\simeq\pi\left|\left\langle n',q'\left|\frac{i}{\hbar}\mathcal{H}_1\right|n,q\right\rangle\right|^2\simeq\pi\delta(q'-q-k)\delta((n'-n)\hbar|\Omega|+\hbar(q'-q)u-\hbar\omega)\times\left|\left\langle\phi_{n',q'}(x)\left|\frac{i}{2\hbar}eV_1\sinh(kx)\right|\phi_{n,q}(x)\right\rangle\right|^2\ . \tag{9}$$

One recognizes inside the δ functions of (9) the energy-momentum conservation laws: the change in the particle total energy and canonical momentum equal the energy and the momentum of a radiation quantum $\mathcal{E}_{n',q'}-\mathcal{E}_{n,q}=\mp\hbar\omega$ and $\hbar q'-\hbar q=\mp\hbar k$, where $-$ $(+)$ corresponds to radiation emission (absorption). Let us now focus on transitions between states of equal cyclotron energy $n'=n$. Energy conservation using (6) yields

$$\mathcal{E}_{n,q'}-\mathcal{E}_{n,q}=(q'-q)\hbar u=-eE_0\delta X=\mp\hbar\omega\ , \tag{10}$$

while momentum conservation from (5) yields

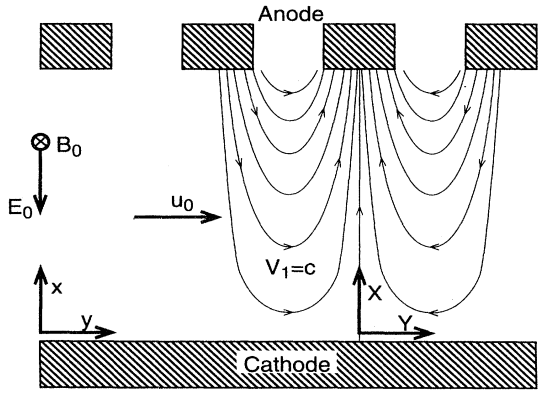

FIG. 2. Simplified drawing of the dc and the ac fields inside a magnetron-type slow-wave cavity. ac equipotentials are plotted in a frame of reference moving at the wave phase velocity $\omega-ku=0$, where the ac field appears as static.

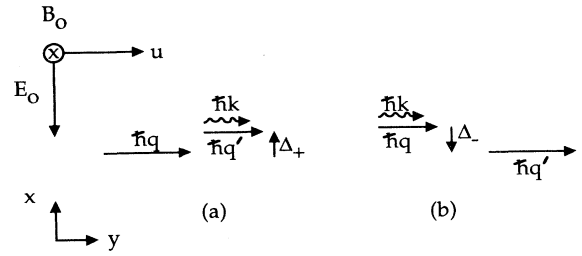

FIG. 3. Sketch of the transverse GC recoil due to momentum conservation during stimulated (a) emission and (b) absorption. Since the **E**×**B** velocity stays constant, the emitted radiation momentum must come from the vector potential of the magnetic field $eA_y/c = m\Omega X$; hence $\Delta_\pm = \pm\hbar\omega/eE_0 = \pm\hbar k/m|\Omega|$.

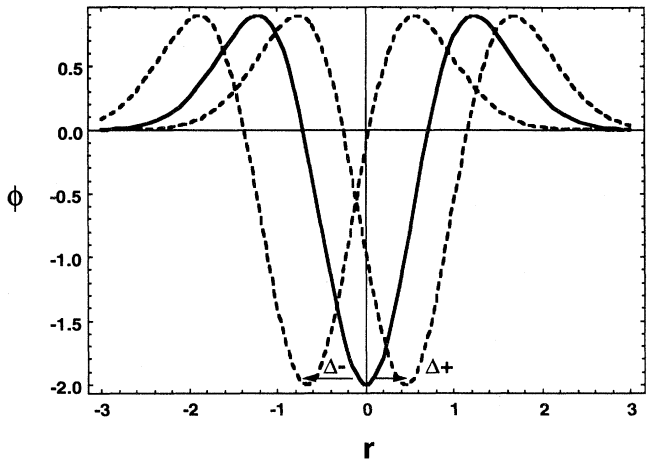

FIG. 4. Wave function $\phi_n(r)$ before (solid) and after (dashed) transition. The state $n=2$ is used for illustration and $r=x-X$ is in units of $\sqrt{\hbar/2m|\Omega|}$. The broken line is the radiation amplitude profile in the vicinity of X (not to scale).

$$\hbar\delta q = m\Omega\delta X = \mp\hbar k \ . \tag{11}$$

From (10) and (11) it follows that the radiative interaction favors synchronous electrons of drift velocity

$$\omega - ku \simeq 0 \ . \tag{12}$$

Conservation of the total momentum Eq. (11), requires that the electron GC recoil by

$$\delta X = \frac{\hbar\delta q}{m\Omega} = \mp\frac{\hbar k}{m\Omega} = \pm\frac{\hbar\omega}{eE_0} \ . \tag{13}$$

The direction of this recoil is perpendicular to the direction of the drift **u** and across the magnetic field, as shown in Fig. 3. The exchanged radiation momentum equals the change in the canonical momentum $\delta P_y = m\Omega\delta X = \delta(eA_y/c)$ stemming from the GC displacement across the vector potential. The exchanged radiation energy equals the change in the electrostatic energy of the electron from the GC shift across the anode-cathode potential. Stimulated emission in crossed E and B fields involves changes in the electrostatic and the vector potentials only. The kinematic energy and momentum remain invariant during the transition.

Whether emitted radiation is amplified depends on the relative strength between absorption and emission probabilities. The per unit time change in the probability amplitude for emission or absorption $X \to X \pm \delta X$ is written in terms of $\delta X = \pm\Delta$ with $\Delta = \hbar\omega/eE_0 = \hbar k/m|\Omega|u$, $r = x - X$, and $r' = x - (X \pm \Delta) = r \mp \Delta$,

$$w_\pm(t) = \left\langle \phi_n(r \mp \Delta) \left| \frac{i}{2\hbar} eV_1 \sinh[k(X+r)] \right| \phi_n(r) \right\rangle \times e^{-i(\omega - ku)t} \ . \tag{14}$$

The terms in angular brackets on the right-hand side is the overlapping integral between initial and final states, illustrated in Fig. 4 for the $n=2$ cyclotron state. Expression (14) is computed by expanding $\phi_n(r \mp \Delta) = \phi_n(r) \mp (d\phi_n/dr)\Delta + \cdots$ and $V_1 \sinh(kx) = V_1 \sinh(kX) + kV_1 \cosh(kX) r + \cdots$. We thus find the total probability $W_\pm(t) \equiv |\int_0^t dt' w_\pm(t')|^2$ for an electron transition in the lower (upper) energy state after time t,

$$W_\pm = \frac{1}{\hbar^2} \left| A\langle\phi_n|\phi_n\rangle \mp A\Delta\langle\phi_n'|\phi_n\rangle + A'\langle\phi_n|r\phi_n\rangle \mp A'\Delta\langle\phi_n'|r\phi_n\rangle + A\frac{\Delta^2}{2}\langle\phi_n''|\phi_n\rangle + \frac{A''}{2}\langle\phi_n|r^2\phi_n\rangle \right|^2 \times \frac{\sin^2[(ku-\omega)t/2]}{[(\omega-ku)/2]^2} \ . \tag{15}$$

Here $A \equiv (eV_1/2)\sinh(kX)$, the prime denotes differentiation with respect to the argument, and we have omitted terms higher than Δ^2 and r^2. The overlapping integrals $\langle\phi_n|r\phi_n\rangle = \langle\phi_n'|\phi_n\rangle = 0$ owing to the odd-even symmetry of $\phi_n(-r) = (-1)^n\phi_n(r)$ and its derivatives under reflection. The remaining contribution is

$$W_{\pm}=\frac{1}{\hbar^2}\left\{A^2+AA''\langle\phi_n|r^2\phi_n\rangle\mp(A^2)'\Delta\langle\phi_n'|r\phi_n\rangle+\frac{\Delta^2}{2}[(A')^2\langle\phi_n'|r\phi_n\rangle^2+2A^2\langle\phi_n''|\phi_n\rangle+AA''\langle\phi_n''|\phi_n\rangle\langle\phi_n|r^2\phi_n\rangle]\right\}\times\frac{\sin^2[(\omega-ku)t/2]}{[(\omega-ku)/2]^2}\ . \tag{16}$$

It follows that the net emission probability $W=W_+-W_-$ is proportional to Δ,

$$W=-\frac{1}{\hbar^2}2\Delta(A^2)'\langle\phi_n'|r\phi_n\rangle t^2 g(\xi)+O(\Delta^3)\ . \tag{17}$$

The line shape function g on the right-hand side is defined in terms of the phase slippage ξ, one-half the product of the frequency detuning $\delta\omega=\omega-ku$ times the transit time t,

$$g(\xi)=\frac{\sin^2\xi}{\xi^2},\quad \xi\equiv\tfrac{1}{2}(\omega-ku)t\ . \tag{18}$$

Terms of the general form $\langle\phi_n^{(k)}|r^m\phi_n\rangle$ are computed using the operator representation of d/dr and r,

$$r=\left[\frac{\hbar}{2m|\Omega|}\right]^{1/2}(a+a^\dagger)\ ,\qquad \frac{d}{dr}=\frac{i}{\hbar}\mathcal{P}_r=\left[\frac{m|\Omega|}{2\hbar}\right]^{1/2}(a-a^\dagger)\ , \tag{19}$$

a and $a^\dagger$ being the Heisenberg operators with the properties $a\phi_n=\sqrt{n}\,\phi_{n-1}$ and $a^\dagger\phi_n=\sqrt{n+1}\,\phi_{n+1}$. Applying (19) to the right-hand side of (17) one finds $\langle\phi_n'|r\phi_n\rangle=-\frac{1}{2}$ and

$$W=\frac{1}{\hbar^2}\Delta(A^2)'g(\xi)+O(\Delta^3)\ . \tag{20}$$

III. COLLECTIVE CHARGE EFFECTS

We have so far ignored the influence of the electrostatic field of the charged electron layer. To take collective beam field into account consider a monolayer of $\mathbf{E}\times\mathbf{B}$ drifting electrons with GC initially located at X. Let the charge density around X, $\rho(r)=\sigma|\Psi(r)|^2$, be a Gaussian of total surface charge density $\int dr\,\rho=\sigma$, where $r=x-X$ as usual. The self-consistent dc potential from $d^2\mathcal{V}_0/dr^2=-4\pi\rho$ is written in a symmetrized form about X as

$$\mathcal{V}_0=-E_0(X+r)-\frac{4\pi\sigma}{\sqrt{\pi}d}\int^r dr'\int^{r'}dr''e^{-(r'')^2/d^2}\ , \tag{21}$$

where $-eE_0(X+r)$ is the unperturbed potential. The system wave function Ψ is then a superposition of eigenstates of various n's,

$$\Psi(r)=\left[\frac{1}{\sqrt{\pi}d}\right]^{1/2}e^{-r^2/2d^2}=\sum_n c_n\tilde{\phi}_n(r)\ , \tag{22}$$

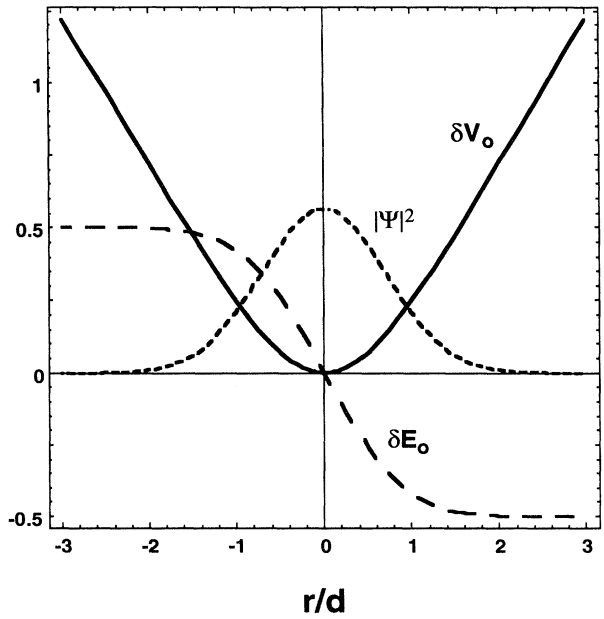

FIG. 5. Charge density and collective dc field around the electron beam.

subject to $\sum_n|c_n|^2=1$. In turn, the presence of the beam field $\delta\mathcal{V}_0$, defined by the integral in Eq. (21) and shown in Fig. 5, modifies the drifting electron eigenstates and eigenvalues $\phi_n\to\tilde{\phi}_n$, $\mathcal{E}_n\to\tilde{\mathcal{E}}_n$. These corrections will contribute to the transition probabilities and the energy balance during emission or absorption.

Up to those point the space-charge thickness d has been arbitrary. Two cases are amenable to analysis. One may consider d either less than the quantum recoil Δ or much larger that the "ground state Larmor radius" $(\hbar/m|\Omega|)^{1/2}$. The narrow Gaussian limit $d<\Delta\le(\hbar/m|\Omega|)^{1/2}$ has been examined elsewhere [12]. Though it is a rather restrictive case, it nevertheless offers a transparent exposition of the underlying physics. Here we take up the more general case $d\gg(\hbar/m|\Omega|)^{1/2}\ge\Delta$.

Consider first the effect of the collective potential $\delta\mathcal{V}_0$ on the drifting electron eigenstates. Since $\delta\mathcal{V}_0(r)$ is independent of y, the renormalized eigenfunctions are given by $\tilde{\psi}_{q,n}(x,y)=e^{iqy}\tilde{\phi}_n(r)$, where

$$\tilde{\mathcal{H}}_0\tilde{\phi}_n\equiv(\mathcal{H}_0+e\delta\mathcal{V}_0)\tilde{\phi}_n(r)=\tilde{\mathcal{E}}_n\tilde{\phi}_n(r)\ . \tag{23}$$

In the small space-charge limit $|\sigma|/E_0\ll1$ one may obtain the perturbed quantities in terms of the vacuum eigenstates via first-order stationary perturbation theory

$$\tilde{\phi}_n(r)=\phi_n(r)-\sum_{m\neq n}\frac{\langle\phi_m|e\delta\mathcal{V}_0|\phi_n\rangle}{\mathcal{E}_m-\mathcal{E}_n}\phi_m(r)\ , \tag{24a}$$

$$\tilde{\mathcal{E}}_n=\mathcal{E}_n+\langle\phi_n|e\delta\mathcal{V}_0|\phi_n\rangle\ . \tag{24b}$$

The results of this computation are given by Eqs. (A17) and (A18) in Appendix A. Notice that $\tilde{\phi}_n(r)$ and $\tilde{\mathcal{E}}_n$ now depend on the GC location $\Delta=X'-X$ relative to the beam center $\Delta=0$.

Now consider transitions among the above eigenstates of $\tilde{H}_0 \equiv H_0 + e\delta\mathcal{V}_0$, induced by the interaction with the wave $H_1 = e\mathcal{V}_1$. The total momentum conservation along y is not affected by $\delta\mathcal{V}_0$, thus relation (13) for the shift in the GC location still holds. The change in $\tilde{\mathcal{E}}_n$, however, affects the energy conservation (10) into

$$\tilde{\mathcal{E}}_{n,q'} - \tilde{\mathcal{E}}_{n,q} = \tilde{\mathcal{E}}_n(\Delta) - \tilde{\mathcal{E}}_n(0) + \hbar u\,\delta q = \mp\hbar\omega \ . \tag{25}$$

To compute $\tilde{\mathcal{E}}_n(\Delta) - \tilde{\mathcal{E}}_n(0)$ notice that the scale length d for the potential $\delta\mathcal{V}_0$ is much larger than the typical wave function width $(\hbar/m|\Omega|)^{1/2}$, thus one may set $e\delta\mathcal{V}_0 \simeq -(e\sigma/\sqrt{\pi}d)r^2$ for the computation of the overlapping integrals in (24). It follows from (A17) and (A22) that

$$\tilde{\mathcal{E}}_n(\Delta) - \tilde{\mathcal{E}}_n(0) = \frac{4\pi e\sigma}{\sqrt{\pi}d} f\frac{\Delta^2}{2}, \quad f \simeq 4 \ . \tag{26}$$

Substitution in the energy balance and use of (11) for δq yields a quadratic for the GC recoil

$$\tfrac{1}{2}m\omega_p^2\Delta^2 - eE_0\Delta \mp \hbar\omega = 0 \ , \tag{27}$$

defining the beam plasma frequency as $\omega_p^2 \equiv f(4\pi e\sigma/\sqrt{\pi}md)$. Thus the dc gradient introduces an asymmetry in the GC jumps between emission and absorption,

$$\Delta_\pm = \pm\frac{\hbar\omega}{eE_0} - \frac{1}{2}\left[\frac{\hbar\omega}{eE_0}\right]^2 \frac{m\omega_p^2}{eE_0} \ . \tag{28}$$

Because $|\Delta_+| < |\Delta_-|$ a stronger overlapping between initial and infal states occurs during emission than absorption, yielding additional contribution to the growth rate.

To compute the transition probability one repeats the procedure of Sec. II using Ψ in lieu of ϕ_n. Only diagonal terms in $n = n'$ are included in $\langle\Psi|e\mathcal{V}_1|\Psi\rangle$ to enforce the no-cyclotron-emission constraint. The result

$$W_\pm = g(\xi)\sum_n |c_n|^2 \left| \left\langle \tilde{\phi}_n(r \mp \Delta) \left| \frac{i}{2\hbar} eV_1 \sinh[k(X+r)] \right| \tilde{\phi}_n(r) \right\rangle \right|^2 \tag{29}$$

is the sum of the transition probabilities for each state times the initial probability of being in that state. The final task is expressing $\langle\tilde{\phi}_n(r\mp\Delta)|e\mathcal{V}_1|\tilde{\phi}_n(r)\rangle$ in terms of $\langle\phi_n(r\mp\Delta)|e\mathcal{V}_1|\phi_n(r)\rangle$. The computation is performed in Appendix B. In the low space charge limit $4\pi\sigma/E_0 = \omega_p^2/\Omega^2 \ll 1$ one finds, keeping terms up to second order in the small parameters Δ, r, and $\beta^2 = \omega_p^2/\Omega^2$,

$$\left\langle \tilde{\phi}_n(r\mp\Delta) \left| \frac{eV_1}{2} \sinh[k(X+r)] \right| \tilde{\phi}_n(r) \right\rangle = \left\langle \phi_n(r\mp\Delta) \left| \frac{eV_1}{2} \sinh[k(X+r)] \right| \phi_n(r) \right\rangle + A\beta_n^2 \ , \tag{30}$$

$$\beta_n^2 = \beta^2[(n+1)^2(n+2)^2 + n^2(n-1)^2] \ .$$

The correction in the transition probability element from the self-field effects is independent of the GC shift $\Delta_\pm$ during the transition. Substituting (30) in (24) and repeating the expansion as after Eq. (14) yields

$$W_\pm = \frac{1}{\hbar^2}\sum_n |c_n|^2 \left\{ A^2 + AA''\langle\phi_n|r^2\phi_n\rangle \mp \Delta_\pm (A^2)'\langle\phi_n'|r\phi_n\rangle \right.$$

$$\left. + \frac{\Delta_\pm^2}{2}[(A')^2\langle\phi_n'|r\phi_n\rangle^2 + 2A^2\langle\phi_n''|\phi_n\rangle + AA''\langle\phi_n''|\phi_n\rangle\langle\phi_n|r^2\phi_n\rangle] + 2A^2\beta_n^2 \right\} t^2 g(\xi) \ . \tag{31}$$

The emission and absorption probabilities are changed by the same amount relative to the zero space-charge result, thus the net emission will be independent of the last term β_n. Using $\sum_n |c_n|^2\langle\phi_n''|\phi_n\rangle = -(m|\Omega|/2\hbar)\sum_n |c_n|^2(2n+1) = -(m|\Omega|/2\hbar)\sum_n |c_n|^2(2\mathcal{E}_n/\hbar|\Omega|) = -(m/\hbar^2)\langle\Psi|\mathcal{H}_0|\Psi\rangle$ and computing $\langle\Psi|\mathcal{H}_0|\Psi\rangle = \frac{1}{2}[(\hbar^2/2md^2) + m\Omega^2 d^2/2]$ directly from $\Psi(r)$ given by (22), one obtains the net emission probability $W \equiv W_+ - W_-$,

$$W = \frac{1}{\hbar^2}\left\{ \frac{\Delta_+ - \Delta_-}{2}(A^2)' + \frac{\Delta_+^2 - \Delta_-^2}{2}\left[(A')^2 - 2A^2\frac{m}{2\hbar^2}\left[\frac{\hbar^2}{2md^2} + \frac{m\Omega^2 d^2}{2} \right] + AA''\sum_n |c_n|^2 (n+\tfrac{1}{2})^2 \right] \right\} t^2 g(\xi) \ . \tag{32}$$

The first contribution from $\Delta_+ - \Delta_- \simeq 2\Delta + O((\sigma/E_0)^2)$ is similar to that in (20). In addition, there is a finite contribution from the quadratic GC recoil term

$$\sum |c_n|^2 \frac{|\Delta_+|^2 - |\Delta_-|^2}{2} \simeq -\sum |c_n|^2 \frac{\hbar^2\omega^3}{e^3 E_0^3} \frac{4\pi\sigma}{\sqrt{\pi} E_0 d} = -\Delta^2 \frac{\omega_p^2 \Delta}{u\Omega} , \tag{33}$$

caused by the space-charge induced asymmetry in the GC shifts for emission or absorption. The last term on the right-hand side of (32) introduces finite Larmor radius effects, since $\sum_n |c_n|^2 (n+\frac{1}{2})^2 = \langle (m\Omega\rho^2/2\hbar)^2 \rangle$. Combining (32) and (33) one finally has

$$W = \frac{1}{\hbar^2} \left\{ \Delta (A^2)' + \Delta^2 \frac{\omega_p^2 \Delta}{u\Omega} \left[A^2 \left[\frac{1}{2d^2} + \frac{m^2\Omega^2 d^2}{2\hbar^2} \right] - (A')^2 - A^2 \left[\frac{m\Omega}{2\hbar} \right]^2 k^2 \langle \rho^4 \rangle \right] \right\} t^2 g(\xi) . \tag{34}$$

IV. RADIATION GAIN

The per-cavity pass radiation gain $G(t)$, determined by the number of photons emitted after a time equal to the cavity transit time $t = L/u$, is equal to the electron flux $(\sigma/e)ub$, b being the width of the beam, times the net emission probability, times the emitted quantum $\hbar\omega$,

$$G(t) = \frac{\sigma}{e} ub [W_+ - W_-] \hbar\omega . \tag{35}$$

Substituting W from Eq. (34) and taking the classical limit $\hbar \to 0$, only the leading-order terms independent of $\hbar$ survive. In the "cold" beam case, implying a Larmor radius much smaller than the wavelength $k^2\langle\rho^2\rangle \to 0$, one obtains

$$\Delta P = \frac{kb}{2} \frac{e\sigma}{m|\Omega|} V_1^2 \left[\sinh(kX)\cosh(kX) + \frac{\sigma}{E_0} \frac{\omega^2}{k^2 u^2} kd\sqrt{\pi} f \sinh^2(kX) \right] \times \omega^2 t^2 g(\xi) . \tag{36}$$

The first and the second terms on the right-hand side of (36) reflect two effects that make the probability for stimulated emission larger than stimulated absorption. First, the rf field strength increases with X and thus favors transitions shifting the GC upwards $\Delta_+ > 0$. That corresponds to electrons falling into lower potential energy state $e\Delta\mathcal{V}_0 = -eE_0\Delta_+ < 0$ via radiation emission. Second, the gradient of the dc field across the electron beam charge causes a stronger initial-field state overlapping during emission, given that the GC displacement is smaller for stimulated emission than absorption, $\Delta_+^2 \propto 1/E_+^2 < \Delta_-^2 \propto 1/E_-^2$.

The radiation gain is defined by $G = \Delta P/P$, where the total radiation power flux in the cavity P is related to the ac amplitude V_1 via the cavity impedance Z by $P = V_1^2/2Z$. It follows from Eq. (36) that

$$G = \frac{\omega}{|\Omega|} \frac{eI_b Z}{2mu^2} \left[\sinh(kx)\cosh(kX) + \frac{\sigma}{E_0} \frac{\omega^2}{k^2u^2} kd\sqrt{\pi} f \sinh^2(kX) \right] \times \omega^2 t^2 g(\xi) , \tag{37}$$

where G is expressed in terms of the beam current $I_b = e\sigma bu$ using $Zkb(e\sigma/m|\Omega|) = (\omega/|\Omega|)(eI_b Z/mu^2)$. Figure 6 shows the gain $\Delta P/P_i$ vs frequency detuning ξ, obtained from (37) over a cavity interaction length of 20 wavelengths for different space-charge densities. The beam thickness is taken to be $\frac{1}{20}$ of the radiation wavelength $kd = 0.1\pi$. The other fixed parameters are $Z = 25$ Ω, $b = 1$ cm, $kX = 1$, and $u/c = 0.0989$, corresponding to a dc electric field $E_0 = 14.84$ kV/cm at $B_0 = 500$ G. The three curves correspond to beam currents I_b equal to 2, 6.6, and 20 mA, respectively, yielding $eI_b Z/mu^2$ from 1×10^{-5} to 1×10^{-4} and σ/E_0 ratios from 4×10^{-5} to 4×10^{-4}. Note that the pure space-charge contribution [the last term on the right-hand side of (37)] becomes important only when $\sigma/E_0 \sim \coth(kX)/\sqrt{\pi}kd$.

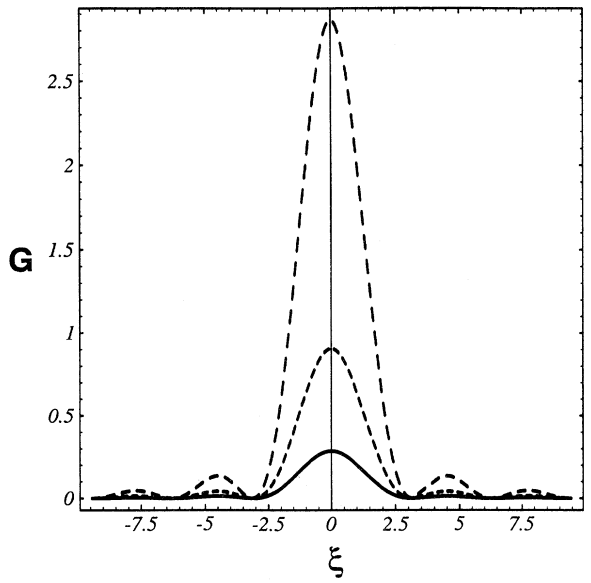

FIG. 6. Pure drift (magnetron) interaction gain vs detuning $\xi = (\omega - ku)L/2u$ for normalized beam currents 1×10^{-5} (solid line), 3.3×10^{-5} (short-dashed line), and 1×10^{-4} (long-dashed line).

The gain formula (37) agrees with recent results [13] derived under the equivalent classical approach. The gain is *symmetric* relative to the resonant frequency $\omega_0 = ku$. Over short times $(\omega - ku)t \ll 1$, $g(\xi) \to t^2$ and the radiation power increases as t^2, independently of the detuning $\delta\omega = \omega - ku$. The gain depends on the transverse gradients $d\mathcal{V}_1/dX$ and $\sigma \propto dE_0/dX$ relative to the wave propagation direction, the emission process being

fundamentally *two dimensional.* Finite Larmor radius effects do not enter directly the energy balance during the emission of a quantum, but affect the local field gradient dE_0/dX and thus the balance between stimulated emission and absorption.

When emission takes place inside cavities with smooth boundaries (diocotron mode limit) the rf profile is given by $\exp(-k|x|)\exp[i(ky-\omega t)]$ instead of (6). The rf field E_1 is antisymmetric around the beam location X, $d\mathcal{V}_1/dX_- + d\mathcal{V}_1/dX_+ = 0$, causing a null contribution from the first term in (37). The instability is then triggered by the second term from the space-charge effects. It must be stressed that since smooth conductive wall cavities do not support slow waves in vacuum, the latter are supported thoroughly by the collective beam plasma modes. In other words, one cannot neglect the ac field of the beam charge perturbation, since it determines the cavity dispersion $\omega(k)$ and the mode structure.

The spectral broadening due to the finite "lifetimes" of the interacting radiation and electron eigenstates is obtained by multiplying (14) with $e^{-\Gamma t/2}$, $1/\Gamma$ being the combined lifetime. The spectral density $\mathcal{U}(\omega)$ of the emitted radiation from the integration $\int_0^\infty dt\, e^{-\Gamma t}[W_+(t) - W_-(t)]$ is

$$\mathcal{U}(\omega) \propto \frac{(\omega - ku)^2}{(\omega - ku)^2 + \Gamma^2} \ . \tag{38}$$

For rf frequencies up to tetrahertz and for beam densities yielding similar plasma frequencies, the spontaneous emission and electron-electron collision effects are negligible. The linewidth Γ is determined by the inverse electron transit time Γ_s through the cavity length L and the inverse cavity decay time ω/Q, $\Gamma^{-1} \simeq \omega/Q + L/u$. Notice the absence of thermal broadening due to velocity spreads. Since the drift velocity u is determined by the field strengths at the GC location X, any velocity spreads among electrons injected at the same GC location must be distributed in their cyclotron rotation velocities. In quantum terms this translates into a spread over the oscillation quantum number n, Eq. (4). The radiation gain (37) is independent of n and thus of thermal spreads.

In the classical treatment the gain is shown to be proportional to the shift in the average GC location of the injected electron cloud [9]. Consider again a monoenergetic electron layer with GC located at $x = X$ and uniformly distributed rf phases $-\pi < ky - \omega t < \pi$. In the electron frame of reference $\omega - ku \simeq 0$ the cavity wave appears as a static potential; the axial ac field causes an $\mathbf{E}_1 \times \mathbf{B}$ drift in the transverse direction, $u_{1x} = E_{1y}/\Omega$. The change in the dc potential energy $e\Delta\mathcal{V}_0 = v_{1x} e E_0 \Delta t$ equals the work done on the ac field $uE_{1y}\Delta t$ since the dc drift velocity u and the cyclotron energy is constant. Initially equal numbers of electrons gain and lose energy and the average upward GC displacement is equal to the average downward displacement. Yet a finite amount of energy is exchanged with the radiation, owing to the jump in the dc field across the electron layer. Over longer times an asymmetry develops in the average GC shift as electrons moving towards the area of higher rf field strength are accelerated, while electrons shifting towards the lower rf field strength are decelerated. The finite shift in the beam center of charge produces a finite energy loss to radiation, even without counting space-charge effects in the dc field.

It is often stated in plasma theory texts that electrons emit or absorb radiation depending on whether they move above or below the wave phase velocity, respectively. That is sometimes misinterpreted as if supersynchronous (subsynchronous) electrons can *only* emit (absorb) radiation; that statement is at odds with the symmetric crossed-field device (CFD) gain, which implies that electrons emit regardless to their velocity relative to the wave. The correct statement is that electrons both emit and absorb regardless of their relative velocity and that under given circumstances the number of quanta emitted may exceed the number of quanta absorbed by a given electron, causing radiation gain, and vice versa. In most UED's the electron recoil makes the emission (absorption) probability higher for electrons above (below) the wave velocity. In CFD's the balance between emission and absorption is not determined by the $\mathbf{E}\times\mathbf{B}$ velocity; the transverse recoil combined with the transverse field gradient causes higher emission rate for all electrons.

V. DRIFT-CYCLOTRON EMISSION

Finally, we consider the effects of cyclotron emission for a monoenergetic drifting beam, by allowing radiative transitions between different oscillator states $\delta n = \pm 1$. The energy levels during transitions are sketched in Fig. 7. The energy-momentum balance gives the new selection rules

$$\hbar\delta q = m\Omega\delta X = \mp\hbar k \ , \tag{39}$$

$$\delta\mathcal{E} = \mp\hbar|\Omega| + \hbar u\,\delta q = \mp\hbar|\Omega| - eE_0\delta X = \mp\hbar\omega \ . \tag{40}$$

Accordingly, emission or absorption now occurs when the Doppler-shifted radiation frequency matches the electron cyclotron frequency

$$\omega - ku = |\Omega| \tag{41}$$

and is again accompanies by a GC shift $\delta X = \pm\Delta$

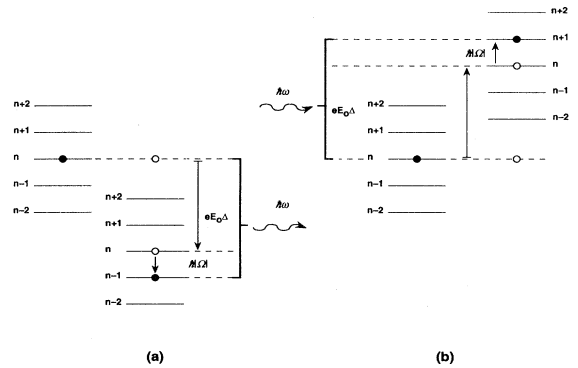

FIG. 7. Energy exchange in the drift-cyclotron emission (fast branch). (a) An increment of electrostatic energy plus a cyclotron rotation quantum are converted into an emitted radiation quantum. (b) The inverse takes place during absorption.

$$\pm\Delta=\pm\frac{\hbar(\omega-|\Omega|)}{eE_0}=\mp\frac{\hbar k}{m\Omega} . \tag{42}$$

The drift kinetic energy and momentum are conserved during transitions. The rate of change of the transition probability amplitude between initial and final states is now given by

$$w_{\pm}(t)=\left\langle\phi_{n\mp1}(r\mp\Delta)\left|\frac{i}{2\hbar}eV_1\sinh[k(X+r)]\right|\phi_n(r)\right\rangle \times e^{-i(\omega-ku-|\Omega|)t} . \tag{43}$$

Repeating the gain computation with (43) in lieu of (14) and neglecting space-charge effects, one finds

$$W_{\pm}=\frac{1}{\hbar^2}\left|A\langle\phi_{n\mp1}|\phi_n\rangle\mp A\Delta\langle\phi'_{n\mp1}|\phi_n\rangle+A'\langle\phi_{n\mp1}|r\phi_n\rangle \mp A'\Delta\langle\phi'_{n\mp1}|r\phi_n\rangle+A\frac{\Delta^2}{2}\langle\phi''_{n\mp1}|\phi_n\rangle+\frac{A''}{2}\langle\phi_{n\mp1}|r^2\phi_n\rangle\right|^2 t^2g(\xi) . \tag{44}$$

Here the phase slippage is expressed in terms of the detuning $\delta\omega=\omega-ku-|\Omega|$ by

$$\xi=\tfrac{1}{2}(\omega-ku-|\Omega|)t . \tag{45}$$

Again, applying the odd-even properties of ϕ_n reduces (44) to

$$W_{\pm}=\frac{1}{\hbar^2}\{A^2\Delta^2\langle\phi'_{n\mp1}|\phi_n\rangle^2+(A')^2\langle\phi_{n\mp1}|r\phi_n\rangle^2 \mp2AA'\Delta\langle\phi'_{n\mp1}|\phi_n\rangle\langle\phi_{n\mp1}|r\phi_n\rangle\}t^2g(\xi) . \tag{46}$$

Computation of the elements

$$\langle\phi'_{n\mp1}|\phi_n\rangle=\sqrt{m|\Omega|/2\hbar}(-\sqrt{n}\,\delta_{n-1,n}+\sqrt{n+1}\delta_{n+1,n})$$

and

$$\langle\phi_{n\mp1}|r\phi_n\rangle=\sqrt{\hbar/2m|\Omega|}(\sqrt{n}\,\delta_{n-1,n}+\sqrt{n+1}\delta_{n+1,n})$$

yields the net gain

$$W=\frac{1}{\hbar^2}\left\{-\frac{1}{2}(A^2)'\Delta-(A')^2\frac{\hbar}{2m|\Omega|} -A^2\Delta^2\frac{m|\Omega|}{2\hbar}\right\}t^2g(\xi) . \tag{47}$$

The first term on the right-hand side of (47) comes from the GC shift and is similar but of opposite sign to the earlier results without cyclotron emission. Pure cyclotron emission effects are expressed by the second term in (47), while the third term carries the cross coupling of the GC shift and the cyclotron emission. All terms in (47) contribute to net absorption of radiation at any frequency mismatch. A nonrelativistic beam near the drift-cyclotron resonance is stable, as opposed to the pure drift resonance instability. This happens because the final electron eigenstate is not only shifted in space by Δ, but also changes to a different eigenfunction $\phi_n\rightarrow\phi_{n+1}$, causing the absorption probability to exceed emission. The reader will recall that nonrelativistic electron cyclotron interaction without the $\mathbf{E}\times\mathbf{B}$ drift also results in a radiation damping (it is always assumed that the radiation amplitude is strong enough so that spontaneous emission is negligible compared to the stimulated emission or absorption).

One must introduce relativistic effects to recover a contribution similar to the usual cyclotron instability. Neglecting electron spin, the relativistic drifting particle Hamiltonian is

$$\hat{\mathcal{H}}_0=mc^2\left[1+\left[\frac{P_x}{mc}\right]^2+\left[\frac{P_x-eA_y/c}{mc}\right]^2\right]^{1/2}-eE_0x \simeq\mathcal{H}_0-\frac{(\mathcal{H}_0+eE_0x)^2}{2mc^2}+mc^2 , \tag{48}$$

where $\mathcal{H}_0$ is the nonrelativistic operator (1). We remaining the slow-wave region $u/c\ll1$, retaining relativistic effects in the transverse motion (cyclotron oscillation). The relativistic energy spectrum (minus the rest energy), computed in Appendix C, is given by

$$\hat{\mathcal{E}}_{n,q}\simeq(n+\tfrac{1}{2})\hbar|\Omega|\left[1-\frac{(n+\frac{1}{2})\hbar|\Omega|}{2mc^2}\right]+\hbar qu-\tfrac{1}{2}mu^2 . \tag{49}$$

According to (49), the relativistic oscillator spectrum is given by $\hat{\mathcal{E}}_n=(n+\frac{1}{2})\hbar|\hat{\Omega}_n|$, where the relativistic cyclotron frequency depends on the energy quantum number n,

$$\hat{\Omega}_n=\Omega\left[1-\frac{(n+\frac{1}{2})\hbar|\Omega|}{2mc^2}\right] . \tag{50}$$

The shift in the cyclotron frequency modifies the wave-particle resonance condition. The energy conservation during transitions dictates that maximum emission or absorption probabilities occur at different frequencies

$$\omega_{\pm}\equiv ku+|\Omega|\left[1-\frac{(n+\frac{1}{2})|\Omega|\hbar}{2mc^2}\right]\mp\frac{\hbar\Omega^2}{2mc^2} =ku+|\hat{\Omega}_n|\mp\frac{\hbar\Omega^2}{2mc^2} . \tag{51}$$

The phase slippage is now given by $\xi=\frac{1}{2}(\omega-ku-|\hat{\Omega}_n| \mp\hbar\Omega^2/2mc^2)t=\xi_n\mp\hbar\Omega^2t/4mc^2$, where $\xi_n\equiv\frac{1}{2}(\omega-ku-|\hat{\Omega}_n|)t$. Thus relativistic effects in the balance between

emission and absorption manifest in two ways: the cyclotron frequency is replaced by its relativistic value $\Omega \rightarrow \hat{\Omega}_n$ and an additional gain contribution results from the difference in the line shape factors $g(\xi) \rightarrow g(\xi_n \mp \hbar\Omega^2 t/4mc^2)$. Expanding

$$g\left[\xi_n \mp \frac{\hbar\Omega^2 t}{4mc^2}\right] = g(\xi_n) \mp \frac{\partial g}{\partial \xi_n}\frac{\hbar\Omega^2 t}{4mc^2}$$

and repeating the transition probability computation of the preceding paragraph one finds

$$\hat{W} = W(\hat{\Omega}_n) + \frac{1}{\hbar^2}\frac{\hbar\Omega^2}{2mc^2}\frac{t}{2}\frac{\partial g}{\partial \xi_n}\{A^2\Delta^2(\langle \phi'_{n-1}|\phi_n\rangle^2 + \langle \phi'_{n+1}|\phi_n\rangle^2) + (A')^2(\langle \phi_{n-1}|r\phi_n\rangle^2 + \langle \phi_{n+1}|r\phi_n\rangle^2) - AA'\Delta(\langle \phi'_{n-1}|\phi_n\rangle\langle \phi_{n-1}|r\phi_n\rangle - \langle \phi'_{n+1}|\phi_n\rangle\langle \phi_{n+1}|r\phi_n\rangle)\} . \quad (52)$$

The first term after the equal sign is given by the right-hand side of Eq. (47) with $\hat{\Omega}_n$ in place of Ω and ξ_n in place of ξ. The large term in curly brackets comes from the shift between the absorption and emission line shapes and reduces to

$$\frac{1}{\hbar^2}\left\{A^2\Delta^2\frac{m|\Omega|}{2\hbar} + (A')^2\frac{\hbar}{2m|\Omega|}\right\}(n+\tfrac{1}{2})\frac{\hbar\Omega^2}{mc^2}\frac{t}{2}\frac{\partial g}{\partial \xi_n} . \quad (53)$$

The relativistic gain contribution depends on the oscillation number n, i.e., the cyclotron rotation energy. The factor $\partial g/\partial \xi_n$ is *antisymmetric* in detuning and *destabilizing* ($\partial g/\partial \xi_n > 0$) for $|\hat{\Omega}_n| > \omega - ku$. The combination of (46) and (53) and the use of the definitions of A and A' finally leads, in the classical limit $\hbar \rightarrow 0$, to

$$\Delta P = kb\frac{e\sigma}{m|\Omega|}V_1^2\left\{-\frac{1}{8}[\sinh(kX)+\cosh(kX)]^2 g(\xi_n) + \frac{1}{8}[\sinh^2(kX)+\cosh^2(kX)] \times (\gamma_n - 1)\frac{|\Omega|t}{2}\frac{\partial g}{\partial \xi_n}\right\}\omega^2 t^2 . \quad (54)$$

The gain is then

$$G = \left[\frac{\omega}{|\Omega|} - 1\right]\frac{eI_b Z}{mu^2} \times \left\{-\frac{1}{8}[\sinh(kX)+\cosh(kX)]^2 g(\xi_n) + \frac{1}{8}[\sinh^2(kX)+\cosh^2(kX)] \times (\gamma_n - 1)\frac{|\Omega|t}{2}\frac{\partial g}{\partial \xi_n}\right\}\omega^2 t^2 . \quad (55)$$

Formula (55) gives the drift-cyclotron gain in a slow-wave cavity for relativistic electrons of "perpendicular" $\gamma_n - 1 = (n+\frac{1}{2})\hbar\Omega^2/mc^2$. It is the counterpart of Eq. (37) for the pure drift gain. Collective space-charge effects have been neglected in the drift-cyclotron treatment.

Figure 8 shows the gain $\Delta P/P_i$ vs frequency detuning for interaction length of 30 wavelengths, $eI_b Z/mu^2 = 1\times10^{-4}$ for $I_b = 20$ mA, and various γ_n. The resonant frequency $\omega = |\Omega|/[1 - u/v_p(\omega)]$ from Eq. (41) corresponds to $\omega = 1.5|\Omega|$ when $u/v_p = uk/\omega = \frac{2}{3}$. For $\gamma_n - 1 = 0$ there is net absorption everywhere in the spectrum (solid line). At $\gamma_n - 1 = 10^{-2}$ there is a small effect on the gain symmetry, yet the gain remains predominantly negative. At $\gamma_n - 1 = 10^{-1}$ the destabilizing relativistic term dominates and strong gain results for $|\Omega_n| > \omega - ku$. From the balance of terms inside (55) one finds the instability condition

$$\gamma_n - 1 > K\frac{2}{|\Omega_n|t}\frac{g}{\partial g/\partial \xi_n} = \frac{K}{|\Omega_n|t}\frac{1}{\cot\xi - 1/\xi} , \quad (56)$$

where $K \equiv [\sinh(kX)+\cosh(kX)]^2/[\sinh^2(kX) + \cosh^2(kX)]$ and $\cot\xi - 1/\xi > 0$. A given γ_n determines the unstable range of frequencies via (56); for strong gain

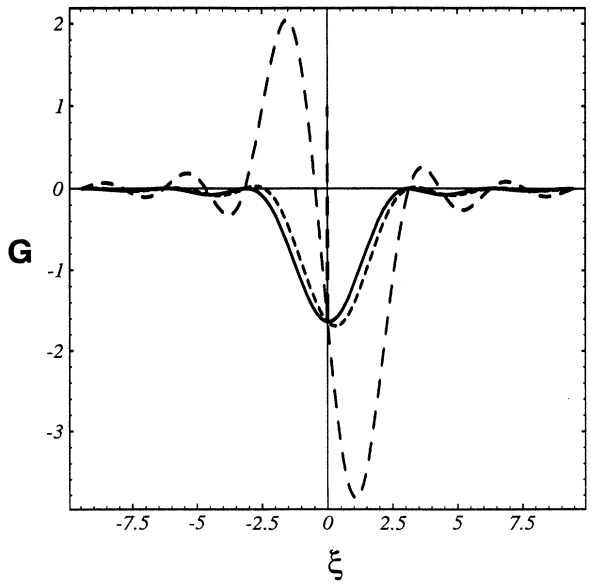

FIG. 8. Fast branch drift-cyclotron gain vs detuning $\xi = (\omega - ku - |\Omega|)L/2u$ for $\gamma - 1 = 3\times10^{-4}$ (solid line), $\gamma - 1 = 3\times10^{-3}$ (short-dashed line), and $\gamma - 1 = 3\times10^{-2}$ (long-dashed line). The normalized beam current $eI_b Z/mu^2$ is 15×10^{-4} and the resonant frequency is 1.5 times the cyclotron.

one must destabilize frequencies near the maximum of $\partial g/\partial \xi$ in Eq. (55), which occurs at $\xi \simeq 1.303$. Letting $\xi \simeq 1.3$ and for $kX \simeq 1$ one obtains from (56) $\gamma_n - 1 \geq 0.373/|\Omega_n| t = 0.373/\omega t(1-u/v_p)$. For typical cavity lengths over ten rf periods and for $u/v_p \simeq \frac{1}{2}$, the threshold in $\gamma_n - 1$ turns out to be less than 10^{-1}.

While the drift-cyclotron case depends strongly on relativistic effects, the pure drift instability, discussed in Secs. III-IV, is insensitive to relativistic effects. The GC shift Δ given by (28) is independent of the relativistic factor γ since $m\omega_p^2$ and $m\Omega$ are relativistically invariant. The gain in (37) is relativistically invariant.

So far we treated the process where a decrement of the electrostatic potential energy plus a cyclotron quantum are converted into a radiation quantum during emission. It is also possible to have an interaction where the decrement in the electrostatic energy is split between the emitted radiation quantum and an *absorbed* oscillation quantum, as in Fig. 9. Here the electrostatic energy is partly converted into radiation and partly going into increasing the cyclotron rotation energy. The analog of the energy conservation equation (40) during emission or absorption now is

$$\delta \mathcal{E} = \pm\hbar|\Omega| + \hbar u\,\delta q = \pm\hbar|\Omega| - eE_0\delta X = \mp\hbar\omega \ . \quad (57)$$

Accordingly, radiative transitions occur when

$$\omega \simeq ku - |\Omega| \quad (58)$$

accompanied by a GC shift $\delta X = \pm\Delta$

$$\pm\Delta = \pm\frac{\hbar(\omega + |\Omega|)}{eE_0} = \mp\frac{\hbar k}{m\Omega} \ . \quad (59)$$

The various interaction modes of a drifting electron beam in a slow-wave cavity are shown in Fig. 10. The intersections of the resonance curve (58) with the waveguide dispersion relation $\omega(k)$ generally correspond to phase velocities lower than (41). Hence (58) characterizes the slow drift-cyclotron branch, as opposed to the fast branch, Eq. (41), discussed earlier in this section.

The slow branch gain is found by observing that the new transition elements for emission and absorption, respectively involving $n+1$ and $n-1$ as final states, are found by exchanging $n \mp 1 \to n \pm 1$ in (43). Hence

$$G = \left[\frac{\omega}{|\Omega|} + 1\right]\frac{eI_b Z}{mu^2}\left\{\frac{1}{8}[\sinh(kX) + \cosh(kX)]^2 g(\xi_n) - \frac{1}{8}[\sinh^2(kX) + \cosh^2(kX)] \times (\gamma_n - 1)\frac{|\Omega| t}{2}\frac{\partial g}{\partial \xi_n}\right\}\omega^2 t^2 \ . \quad (60)$$

The cyclotron emission contributions enter the gain with reversed sign relative to (55). Thus the nonrelativistic, slow drift-cyclotron branch is always unstable, in contrast to the stability of its fast counterpart. The relativistic contribution, proportional to $\partial g(\xi_n)/\partial \xi_n$, is antisymmetric relative to the detuning $\delta\omega = \omega - ku + |\hat{\Omega}_n|$ and *stabilizing* when $|\hat{\Omega}_n| > ku - \omega$. Figure 11 shows the gain $\Delta P/P_i$ vs frequency detuning for interaction length of 30 wavelengths, $eI_b Z/mu^2 = 2\times 10^{-5}$ for $I_b = 4mA$, and various γ_n. The resonant frequency $\omega = |\Omega|/[u/v_p(\omega) - 1]$ from Eq. (58) corresponds to $\omega = 4|\Omega|$ for $u/v_p = uk/\omega = \frac{5}{4}$. For $\gamma_n - 1 = 0$ there is instability everywhere in the spectrum (solid line). For $\gamma_n - 1 = 10^{-1}$ (long-dashed line) there is a relativistic stabilization of some frequencies in the range $|\hat{\Omega}_n| > ku - \omega$.

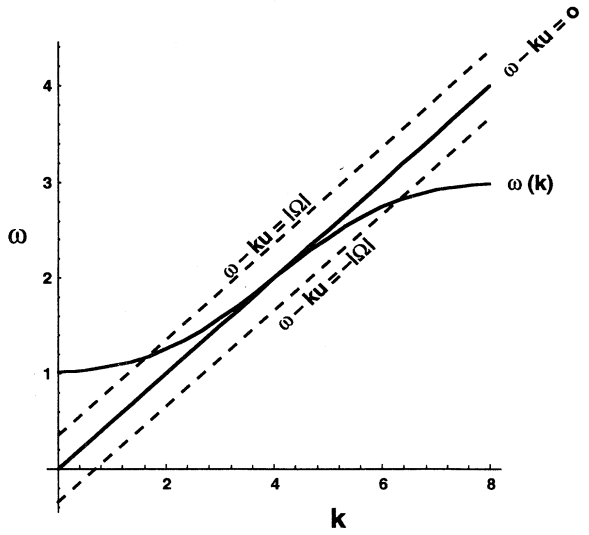

FIG. 10. Slow cavity mode amplification by E×B drifting beams. Possible operation points are located near the intersections of the magnetron, drift-cyclotron, and slow drift-cyclotron resonances with the cavity dispersion $\omega(k)$ (only the first Brillouin zone of the latter is shown).

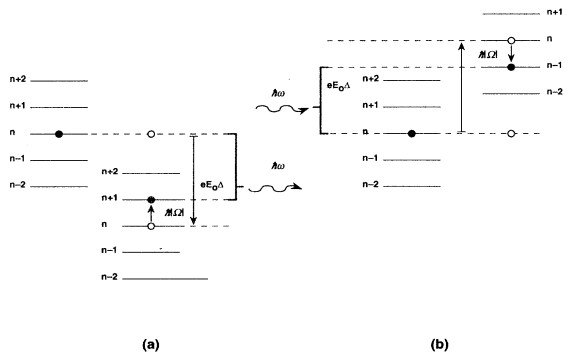

FIG. 9. Energy exchange in the drift-cyclotron emission (slow branch). (a) An increment of electrostatic energy minus an *absorbed* cyclotron quantum is converted into an emitted radiation quantum. (b) The inverse takes place during absorption.

VI. CONCLUSIONS

Microwave amplification by stimulated emission from E×B drifting electrons in slow-wave cavities can occur when the Doppler shifted wave frequency $\omega - ku$ is either near zero or near the cyclotron frequency. The synchro-

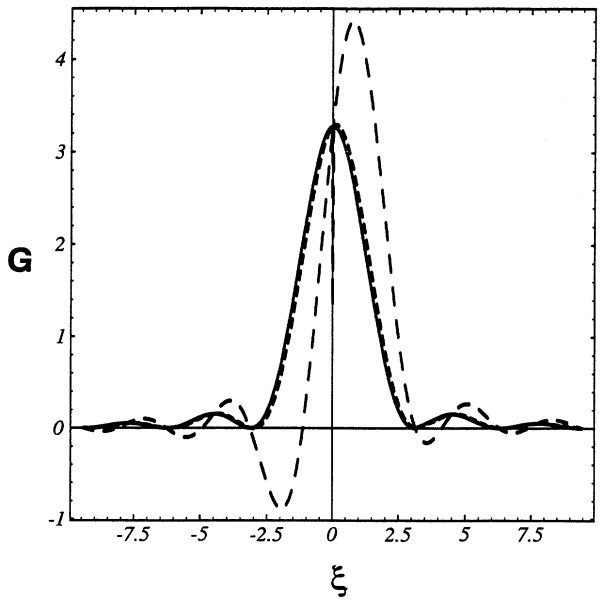

FIG. 11. Slow branch drift-cyclotron gain vs detuning $\xi=(\omega-ku+|\Omega|)L/2u$ for $\gamma-1=3\times10^{-4}$ (solid line), $\gamma-1=3\times10^{-3}$ (short-dashed line), and $\gamma-1=3\times10^{-2}$ (long-dashed line). The normalized beam current eI_bZ/mu^2 is 2×10^{-5} and the resonant frequency is 4 times the cyclotron.

nous beam case $\omega-ku\simeq0$, termed the pure drift instability, is always unstable to microwave growth. This instability is underlying the magnetron operation where the synchronism is referred to as the Buneman-Hartree condition. The gain is symmetric in respect to the detuning $|\delta\omega|=|\omega-ku|$ and independent of the cyclotron energy. The energy and the momentum of the emitted radiation come from the changes in the electrostatic potential and vector potential of the electrons, associated with the external electric and magnetic field. The electron drift kinetic and cyclotron energies are invariant during the radiative transitions. The GC recoil is perpendicular to the direction of emission. The gain is expressed via a general initial-final transition probability amplitude $w=\hbar^{-1}\langle\phi_n|e\mathcal{V}_1|\phi_n\rangle$, where the slow-wave ac potential $\mathcal{V}_1(x,y,t)$ can assume the structure appropriate to any waveguide, not necessarily limited to (7). If F is the number flux of electrons in a sheet beam of surface charge density σ passing through X, the small amplitude gain formula is

$$G=FZ\left[\Delta\frac{\partial|w|^2}{\partial X}+\left[\sigma\frac{\partial\Delta^2}{\partial\sigma}\right]\frac{1}{2}\left|w\frac{\partial^2 w}{\partial X^2}\right|\right]g(\xi)\hbar\omega\ . \quad (61)$$

The first term on the right-hand side is proportional to the recoil distance, times the spatial derivative of w^2 stemming from the transverse gradients in the ac field strengths. Collective space-charge effects carried be the second term are proportional to the asymmetry in the GC shift caused by the dc field gradients. Formula (61) does not depend on the relativistic factor γ since cyclotron emission is frozen during the process and Δ turns out relativistically invariant. Finite Larmor radius effects manifest indirectly, via the collective fields; the cyclotron radius affects the charge distribution σ and the local field gradients about the GC location.

In the drift-cyclotron resonance $\omega-ku\simeq\pm|\Omega|$, the emitted radiation energy comes from the shift in the electron GC location and the change in the cyclotron radiation energy. The drift kinetic energy and momentum are still invariant during transitions. Two cases occur: a subsynchronous beam interacting with the fast branch $v_p(\omega)>u=\omega/k-|\Omega|/k$ and a supersynchronous beam with the slow branch $v_p(\omega)<u=\omega/k+|\Omega|/k$. In the nonrelativistic region $(n+\frac{1}{2})\hbar|\Omega|/mc^2\to0$ the gain remains symmetric relative to the detuning $\delta\omega=\omega-ku\mp|\Omega|$ and of the general form

$$G=FZ\left[-\Delta^2\left|\frac{\partial w}{\partial X}\right|^2-\Delta\left|\frac{\partial w^2}{\partial X}\right|-|w^2|\right]g(\xi)\hbar\omega\ . \quad (62)$$

Here the probability amplitude is of the general form $w=\hbar^{-1}\langle\phi_{n\mp1}|e\mathcal{V}_1|\phi_n\rangle$ and involves transitions between cyclotron states. The nonrelativistic fast branch, involving emission of a cyclotron quantum, turns out stable (the absorption probability of an oscillation quantum exceeds that for emission). The slow branch, involving absorption of a cyclotron quantum during radiation emission, is unstable. Neglecting space-charge effects the gain is independent of the Larmor radius (i.e., quantum number n); it is the same for warm beams $n\neq0$ and cold beams $n=0$.

When the cyclotron rotation energy is in the relativistic range a new contribution arises in the gain from the dependence of the cyclotron rotation frequency on energy $\Omega\to\hat{\Omega}_n$,

$$G=FZ\left[-\Delta_n^2\left|\frac{\partial w_n}{\partial X}\right|^2-\Delta_n\left|\frac{\partial w_n^2}{\partial X}\right|-|w^2|\right]g(\xi_n)\hbar\omega$$
$$+FZ\left[w_n^2+\Delta_n^2\left|\frac{\partial w_n}{\partial X}\right|^2\right](\gamma_n-1)\frac{|\Omega|t}{2}\frac{\partial g(\xi_n)}{\partial\xi_n}\hbar\omega\ . \quad (63)$$

The relativistic contribution from the second term in large square brackets is antisymmetric in detuning. Relativistic effects are destabilizing for the fast branch (stabilizing for the slow branch) in the range $|\Omega_n|>\omega-ku$. Note that in the relativistic case the gain depends explicitly on the cyclotron energy. The growth rate in that case is affected by the spread in the injected electron energies (beam "temperature"). When the relativistic effects dominate, the familiar form of the electron cyclotron maser antisymmetric gain curve shape emerges.

So far, to the best of the author's knowledge, the operation of the crossed-field microwave devices has been based exclusively in the pure drift instability $\omega-ku=0$ (the Buneman-Hartree condition). Despite the high efficiencies achieved in magnetrons note that the energy stored into the cyclotron motion remains untapped. Classical nonlinear gain computations show that it is the Larmor radius that sets the upper limit in the efficiency

$\eta \simeq 1-2\rho/D$, where D is the anode-cathode spacing. The efficiency is thus limited considerably in cases with highly cycloidal electron orbits, as, for example, during secondary or thermionic emission from the cathode. Operation in the fast drift-cyclotron branch converts both electrostatic and cyclotron energies into radiation and should increase efficiency in mildly relativistic magnetrons. Destabilization of the fast cyclotron branch would require typical cyclotron energies of $\gamma_n - 1$ less than 0.1.

The slow drift-cyclotron branch is unstable at arbitrary low γ. For given drift velocity u, a crossed-field amplifier operating at the slow branch can achieve higher frequencies than the usual fast branch. A price will be paid in efficiency since part of the released electrostatic energy is channeled into increasing the cyclotron rotation energy.

A final note is in order, concerning emission at drift-cyclotron *harmonics* $\omega - ku = \pm l|\Omega|$, where $l \geq 2$. This case is of interest because it allows higher frequency generation

$$\omega \simeq \frac{l|\Omega|}{|u/v_p(\omega)-1|}$$

for given $\mathbf{E}\times\mathbf{B}$ velocity u. The amplitude of the transition probability is again proportional to $w = \hbar^{-1}\langle \phi_{n\pm l}|e\mathcal{V}_1|\phi_n\rangle$. It can be shown that the only gain contributions that survive in the classical limit $\hbar \to 0$ scale as $(k\rho_n)^{2l}$. Thus excitation of drift-cyclotron harmonics is significant only when the Larmor radius is comparable to the wavelength. The analysis in this paper focused on the "cold-beam" cases where the Larmor radius, though finite, remained much smaller than the wavelength $(k\rho_n) \ll 1$. Finite Larmor radius effects $\sim (k\rho_n)^2$ can be neglected for $l = \pm 1$; the gain for the fundamental drift-cyclotron branches, given by Eqs. (37) and (55), is dominated by the contributions from the GC shift Δ during transitions.

ACKNOWLEDGMENTS

The author wants to thank D. Chernin and Y. Y. Lau for useful discussions. This work is supported by NRL Contract No. N00014-92-C-2030.

APPENDIX A: SPACE CHARGE EFFECTS ON DRIFTING ELECTRON EIGENSTATES

The dc field resulting from the beam charge affects the electron eigenfunctions and energy eigenvalues. When the space charge is so small as to be negligible the drifting electron wave functions are eigenstates of the operator

$$\mathcal{H}_0\psi_{n,q} = \mathcal{E}_{n,q}\psi_{n,q} , \tag{A1}$$

where the energy is expressed in terms of the "good" (i.e., conserved) quantum numbers as

$$\mathcal{E}_{n,q} = (n+\tfrac{1}{2})\hbar\Omega + \hbar q u - \tfrac{1}{2}mu^2 . \tag{A2}$$

The eigenvalue equation for drifting electrons including the action of the beam self-field is

$$\tilde{\mathcal{H}}_0\tilde{\psi}_{n,q} = \tilde{\mathcal{E}}_{n,q}\tilde{\psi}_{n,q} , \tag{A3}$$

where

$$\tilde{\mathcal{H}}_0 = \mathcal{H}_0 + e\delta\mathcal{V}_0 , \tag{A4}$$

$$\delta\mathcal{V}_0 = -4\pi\sigma\int^r dr'\int^{r'} dr''|\Psi(r'')|^2 = -\frac{4\pi\sigma}{\sqrt{\pi}d}\int^r dr'\int^{r'} dr'' e^{-(r'')^2/d^2} , \tag{A5}$$

and $r = x - X$ is the distance from the beam center X. Since $\delta\mathcal{V}_0$ is independent of y, only the x dependence of $\tilde{\psi}$ is affected by space-charge effects

$$\tilde{\psi}_{n,q}(x,y) = e^{iqy}\tilde{\phi}_n(x) , \tag{A6}$$

where

$$\left[-\frac{\hbar^2}{2m}\frac{d^2}{dr^2} + \frac{1}{2}m\Omega^2 r^2 + e\delta\mathcal{V}_0\right]\tilde{\phi}_n = \tilde{\mathcal{E}}_n\tilde{\phi}_n . \tag{A7}$$

In the small space-charge limit the perturbed $\tilde{\mathcal{E}}_n$ and $\tilde{\phi}_n$ are obtained from the unperturbed $\mathcal{E}_n$ and ϕ_n, solutions of Eq. (2), via stationary perturbation theory. The picture of $\mathbf{E}\times\mathbf{B}$ drifting electrons oscillating about some GC location X' is retained, but now the wave function structure around X' and the oscillator energy are both affected by the location of X' relative to the injected beam center X. Since emission or absorption shifts the guiding center by $\Delta = X' - X$ one must allow the perturbed eigenstates to depend on Δ as well,

$$\tilde{\phi}_n(r' = x - X') = \tilde{\phi}_n(r + X - X') = \tilde{\phi}_n(r \mp \Delta) . \tag{A8}$$

The perturbative expansion up to first order in $\delta\mathcal{V}_0$ is

$$\tilde{\phi}_n(r\mp\Delta) = \phi_n(r\mp\Delta) - \sum_{m\neq n}\frac{\langle \phi_m(r\mp\Delta)|e\delta\mathcal{V}_0|\phi_n(r\mp\Delta)\rangle}{\mathcal{E}_m - \mathcal{E}_n}\times\phi_m(r\mp\Delta) , \tag{A9}$$

$$\tilde{\mathcal{E}}_n = \mathcal{E}_n + \langle \phi_n(r\mp\Delta)|e\delta\mathcal{V}_0|\phi_n(r\mp\Delta)\rangle . \tag{A10}$$

Expanding $\phi_n(r\mp\Delta) \simeq \phi_n(r) \mp \phi_n'\Delta + \phi_n''(\Delta^2/2)$ and using the odd-even symmetry properties of $\phi_n(r)$ and its derivatives under reflection $r \to -r$, as well as the fact the $\delta\mathcal{V}_0$ is even in r, it follows that

$$\tilde{\mathcal{E}}_n(\Delta) = \mathcal{E}_n + \langle \phi_n(r)|e\delta\mathcal{V}_0|\phi_n(r)\rangle + \Delta^2\{\langle \phi_n'(r)|e\delta\mathcal{V}_0|\phi_n'(r)\rangle + \tfrac{1}{2}\langle \phi_n''(r)|e\delta\mathcal{V}_0|\phi_n(r)\rangle + \tfrac{1}{2}\langle \phi_n(r)|e\delta\mathcal{V}_0|\phi_n''(r)\rangle\} , \tag{A11}$$

$$\tilde{\phi}_n(r\mp\Delta)=\phi_n(r\mp\Delta)-\sum_{m\neq n}\frac{\phi_m(r\mp\Delta)}{(m-n)\hbar\Omega}\left\{\langle\phi_m(r)|e\delta\mathcal{V}_0|\phi_n(r)\rangle\mp\Delta[\langle\phi'_m(r)|e\delta\mathcal{V}_0|\phi_n(r)\rangle\mp\langle\phi'_m(r)|e\delta\mathcal{V}_0|\phi_n(r)\rangle]\right.$$
$$\left.+\frac{\Delta^2}{2}[\langle\phi''_m(r)|e\delta\mathcal{V}_0|\phi_n(r)\rangle+2\langle\phi'_m(r)|e\delta\mathcal{V}_0|\phi'_n(r)\rangle+\langle\phi_m(r)|e\delta\mathcal{V}_0|\phi''_n(r)\rangle]\right\}. \tag{A12}$$

Because the scale length d of the potential $\delta\mathcal{V}_0$ is taken much longer than the typical wave function "size" $d\gg\sqrt{\hbar/2m\Omega}$ one may approximate

$$e\delta\mathcal{V}_0\simeq-e\frac{4\pi\sigma}{\sqrt{\pi}d}r^2, \tag{A13}$$

inside the overlapping integrals (A11) and (A12). Expressing r in terms of the ladder operators a and $a^\dagger$ of Eq. (13) yields

$$\langle\phi_m(r)|r^2|\phi_n(r)\rangle=\frac{\hbar}{2m\Omega}\langle\phi_m(r)|(a+a^\dagger)^2|\phi_n(r)\rangle=\frac{\hbar}{2m\Omega}[n(n-1)\delta_{m,n-2}+(n+1)(n+2)\delta_{m,n+2}+\delta_{m,n}], \tag{A14}$$

$$\langle\phi'_m(r)|r^2|\phi_n(r)\rangle+\langle\phi_m(r)|r^2|\phi'_n(r)\rangle=\left[\frac{\hbar}{2m\Omega}\right]^{1/2}\langle\phi_m(r)|(a^\dagger-a)(a+a^\dagger)^2+(a+a^\dagger)^2(a-a^\dagger)\phi_n(r)\rangle$$
$$=\left[\frac{\hbar}{2m\Omega}\right]^{1/2}[-(2n+1)\sqrt{n}\,\delta_{m,n-1}-(2n+3)\sqrt{n}\,\delta_{m,n+1}], \tag{A15}$$

$$\langle\phi'_m(r)|r^2|\phi'_n(r)\rangle=\frac{\hbar}{2m\Omega}\frac{m\Omega}{2\hbar}\langle\phi_m(r)|(a^\dagger-a)(a+a^\dagger)^2(a-a^\dagger)|\phi_n(r)\rangle$$
$$=\tfrac{1}{4}\{[n^2+n(n-1)-(n+1)(n+2)]\delta_{m,n}+2\sqrt{n(n-1)}\delta_{m,n-2}+2\sqrt{(n+1)(n+2)}\delta_{m,n+2}$$
$$-\sqrt{(n+1)(n+2)(n+3)(n+4)}\delta_{m,n+4}+\sqrt{n(n-1)(n-2)(n-3)}\delta_{m,n-4}\}, \tag{A16}$$

$$\langle\phi_m(r)''|r^2|\phi_n(r)\rangle=\frac{\hbar}{2m\Omega}\frac{m\Omega}{2\hbar}\langle\phi_m(r)|(a^\dagger-a)^2(a+a^\dagger)^2|\phi_n(r)\rangle$$
$$=\tfrac{1}{4}\{[n(n-1)+(n+1)(n+2)-(2n+1)^2]\delta_{m,n}-4\sqrt{n(n-1)}\delta_{m,n-2}-4\sqrt{(n+1)(n+2)}\delta_{m,n+2}$$
$$+\sqrt{(n+1)(n+2)(n+3)(n+4)}\delta_{m,n+4}-\sqrt{n(n-1)(n-2)(n-3)}\delta_{m,n-4}\}. \tag{A17}$$

Substituting (A13) into (A11) and (A12) and using the results (A14)–(A17) for the various expectation values yields

$$\tilde{\mathcal{E}}_n(\Delta)=\mathcal{E}_n-\frac{4\pi e\sigma}{\sqrt{\pi}d}\frac{(2n+1)\hbar}{2m\Omega}-\frac{4\pi e\sigma}{\sqrt{\pi}d}\Delta^2\frac{n^2+2n(n-1)-(2n+1)^2}{4}, \tag{A18}$$

$$\tilde{\phi}_n(r\mp\Delta)=\phi_n(r\mp\Delta)-\frac{4\pi e\sigma}{\sqrt{\pi}dm\Omega^2}\tfrac{1}{4}[(n+1)(n+2)\phi_{n+2}(r\mp\Delta)-n(n-1)\phi_{n-2}(r\mp\Delta)]$$
$$\pm\frac{4\pi e\sigma}{\sqrt{\pi}d}\left[\frac{\hbar}{2m\Omega}\right]^{1/2}\frac{\Delta}{\hbar\Omega}[-(2n+1)\sqrt{n}\,\phi_{n-1}(r)+(2n+3)\sqrt{n}\,\phi_{n+1}(r)]$$
$$-\frac{4\pi e\sigma}{\sqrt{\pi}d}\frac{\Delta^2}{4\hbar\Omega}\{\sqrt{n(n-1)}\phi_{n-2}(r)-\sqrt{(n+1)(n+2)}\phi_{n+2}(r)$$
$$+\tfrac{1}{2}\sqrt{n(n-1)(n-2)(n-3)}\phi_{n-4}(r)-\tfrac{1}{2}\sqrt{(n+1)(n+2)(n+3)(n+4)}\phi_{n+4}(r)\}, \tag{A19}$$

The wave function correction in (A19) will be used in the transition probability computation. The last term in (A18), coming from $-\langle\phi'_n|r^2|\phi'_n\rangle-\langle\phi''_n|r^2|\phi_n\rangle$, overestimates the energy shift at large n. The approximation $\mathcal{V}_0\propto r^2$ fails above $r>d$, where the potential asymptotes to a linear increase (Fig. 5) and the eigenfunctions ϕ_n extend beyond d for n large. To make up for the overestimate one may use the ensemble averaged value

$$\sum_n|c_n|^2[\langle\phi'_n|r^2|\phi'_n\rangle+\langle\phi''_n|r^2|\phi_n\rangle]$$
$$=\langle\Psi'|r^2|\Psi'\rangle+\langle\Psi''|r^2|\Psi\rangle, \tag{A20}$$

independently of n. Direct computation of (A20) using (22) for $\Psi(r)$ yields

$$\int_{-\infty}^{\infty} dr\, r^2[\Psi'\Psi'+\Psi''\Psi] = \frac{2}{\sqrt{\pi}d}[\Psi'\Psi r^2-(\Psi^2)'r]_0^{\infty} - \frac{2}{\sqrt{\pi}d}\int_0^{\infty} dr\, e^{-r^2/d^2}=2 . \tag{A21}$$

Thus, from (A18), one arrives at

$$\tilde{\mathcal{E}}_n(\Delta)=\mathcal{E}_n-\frac{4\pi e\sigma}{\sqrt{\pi}d}\frac{(2n+1)\hbar}{2m\Omega}+\frac{4\pi e\sigma}{\sqrt{\pi}d}f\frac{\Delta^2}{2}, \quad f\simeq 4 . \tag{A22}$$

APPENDIX B: TRANSITION PROBABILITY COMPUTATION INCLUDING COLLECTIVE FIELD EFFECTS

The transition probability, given by Eq. (29), involves overlapping between initial and final states of the general form

$$\left\langle \tilde{\phi}_n(r\mp\Delta)\left|\frac{eV_1}{2}\sinh[k(X+r)]\right|\tilde{\phi}_n(r)\right\rangle , \tag{B1}$$

where $\tilde{\phi}_n(r)$ are the modified by the space-charge oscillator wave functions. According to (A14) one may set

$$\tilde{\phi}_n(r)=\phi_n(r)+\delta\phi_n(r) , \tag{B2}$$

where, defining the beam plasma frequency as $\omega_p^2\equiv f(4\pi e\sigma/\sqrt{\pi}md)$ and $\beta\equiv\omega_p^2/\Omega^2$,

$$\begin{aligned}\delta\phi_n(r)=&-\frac{\beta}{4}[(n+1)(n+2)\phi_{n+2}(r)-n(n-1)\phi_{n-2}(r)]\\ &\pm\beta\left[\frac{m|\Omega|}{2\hbar}\right]^{1/2}\Delta[-(2n+1)\sqrt{n}\,\phi_{n-1}(r)+(2n+3)\sqrt{n}\,\phi_{n+1}(r)]\\ &-\beta\frac{m\Omega^2\Delta^2}{4\hbar\Omega}\{\sqrt{n(n-1)}\phi_{n-2}(r)-\sqrt{(n+1)(n+2)}\phi_{n+2}(r)+\tfrac{1}{2}\sqrt{n(n-1)(n-2)(n-3)}\phi_{n-4}(r)\\ &-\tfrac{1}{2}\sqrt{(n+1)(n+2)(n+3)(n+4)}\phi_{n+4}(r)\} .\end{aligned} \tag{B3}$$

To keep terms up to second order in the small parameters Δ, β, and $r<d$ inside the transition elements (B1) one can discard terms $O(\Delta^2)$ on the right-hand side of (B3). Combining (B1) and (B3) then yields

$$\begin{aligned}&\left\langle \tilde{\phi}_n(r\mp\Delta)\left|\frac{eV_1}{2}\sinh[k(X+r)]\right|\tilde{\phi}_n(r)\right\rangle\\ &=\left\langle \phi_n(r\mp\Delta)\left|\frac{eV_1}{2}\sinh[k(X+r)]\right|\phi_n(r)\right\rangle\\ &\quad+\frac{\beta}{4}\left\{\left\langle \phi_n(r\mp\Delta)\left|\frac{eV_1}{2}\sinh[k(X+r)]\right|[(n+1)(n+2)\phi_{n+2}(r)-n(n-1)\phi_{n-2}(r)]\right\rangle\right.\\ &\qquad\left.+\left\langle[(n+1)(n+2)\phi_{n+2}(r\mp\Delta)-n(n-1)\phi_{n-2}(r\mp\Delta)]\left|\frac{eV_1}{2}\sinh[k(X+r)]\right|\phi_n(r)\right\rangle\right\}\\ &\quad+\beta\Delta\left[\frac{m|\Omega|}{\hbar}\right]^{1/2}\left\{\left\langle \phi_n(r\mp\Delta)\left|\frac{eV_1}{2}\sinh[k(X+r)]\right|[(2n+3)\sqrt{n}\,\phi_{n+1}(r)-(2n+1)\sqrt{n}\,\phi_{n-1}(r)]\right\rangle\right.\\ &\qquad\left.+\left\langle[(2n+3)\sqrt{n}\,\phi_{n+1}(r\mp\Delta)-(2n+1)\sqrt{n}\,\phi_{n-1}(r\mp\Delta)]\left|\frac{eV_1}{2}\sinh[k(X+r)]\right|\phi_n(r)\right\rangle\right\}\\ &\quad+\frac{\beta^2}{16}\left\langle[(n+1)(n+2)\phi_{n+2}(r\mp\Delta)\right.\\ &\qquad\left.-n(n-1)\phi_{n-2}(r\mp\Delta)]\left|\frac{eV_1}{2}\sinh[k(X+r)]\right|[(n+1)(n+2)\phi_{n+2}(r)-n(n-1)\phi_{n-2}(r)]\right\rangle .\end{aligned} \tag{B4}$$

The first term on the right-hand side of (B4) is the transition probability for the unperturbed (vacuum) eigenstates and has been computed in Sec. II. The additional contributions on the right-hand side of (B4) are expanded according to

$$\mp\Delta\beta\{(n+1)(n+2)[\langle\phi'_n|A|\phi_{n+2}\rangle+\langle\phi_n|A|\phi'_{n+2}\rangle]-n(n-1)[\langle\phi'_n|A|\phi_{n-2}\rangle+\langle\phi_n|A|\phi'_{n-2}\rangle]\}$$
$$+\beta\{(n+1)(n+2)\langle\phi_n|A'r|\phi_{n+2}\rangle-n(n-1)\langle\phi_n|A'r|\phi_{n-2}\rangle\}$$
$$\mp\beta\Delta\left[\frac{m|\Omega|}{\hbar}\right]^{1/2}\{-(2n+1)\sqrt{n}\,[\langle\phi_n|A|\phi_{n-1}\rangle+\langle\phi_{n-1}|A|\phi_n\rangle]+(2n+3)\sqrt{n}\,[\langle\phi_n|A|\phi_{n+1}\rangle+\langle\phi_{n+2}|A|\phi_n\rangle]\}$$
$$+\beta^2\{(n+1)^2(n+2)^2\langle\phi_{n+2}|A|\phi_{n+2}\rangle+n^2(n-1)^2\langle\phi_{n-2}|A|\phi_{n-2}\rangle\}$$
$$-n(n-1)(n+1)(n+2)\langle\phi_{n+2}|A|\phi_{n-2}\rangle-n(n-1)(n+1)(n+2)\langle\phi_{n-2}|A|\phi_{n+2}\rangle\ , \quad \text{(B5)}$$

where, as usual, $A\equiv(eV_1/2)\sinh X$ and the prime denotes differentiation with respect to the argument. Applying the selection rules inside (B5) and substituting the surviving terms back into (B4) yields

$$\left\langle\tilde{\phi}_n(r\mp\Delta)\left|\frac{eV_1}{2}\sinh[k(X+r)]\right|\tilde{\phi}_n(r)\right\rangle$$
$$=\left\langle\phi_n(r\mp\Delta)\left|\frac{eV_1}{2}\sinh[k(X+r)]\right|\phi_n(r)\right\rangle$$
$$+\beta^2A[(n+1)^2(n+2)^2+n^2(n-1)^2]\ . \quad \text{(B6)}$$

The correction in the transition probability element from the self-field effects is independent of the GC shift $\Delta_\pm$ during the transition. Both the total emission and the total absorption probability are changed by the same amount

$$\beta^2A\sum_{n=0}^{\infty}|c_n|^2[(n+1)^2(n+2)^2+n^2(n-1)^2] \quad \text{(B7)}$$

relative to the zero space-charge result Eq. (14). Thus the net emission probability W_+-W_- is still given (16) using different $\Delta_\pm$ for emission or absorption. The space-charge influence enters through the GC shift: because of the self-field $|\Delta_+|\neq|\Delta_-|$. This causes an additional contribution to the emission probability from the quadratic difference $\Delta_+^2-\Delta_-^2\neq0$, Eq. (32).

APPENDIX C: RELATIVISTIC ENERGY SPECTRUM

The lowest-order expansion of the relativistic drifting electron Hamiltonian is

$$\hat{\mathcal{H}}=mc^2\left[1+\left[\frac{P_x}{mc}\right]^2+\left[\frac{P_x-(e/c)A_y}{mc}\right]^2\right]^{1/2}+e\mathcal{V}_0$$
$$\simeq mc^2+\frac{1}{2m}\left[P_x^2+\left[P_x-\frac{e}{c}A_y\right]^2\right]-eE_0x$$
$$-\frac{mc^2}{8}\left[\left[\frac{P_x}{mc}\right]^2+\left[\frac{P_x-(e/c)A_y}{mc}\right]^2\right]^2$$
$$=mc^2+\mathcal{H}-\frac{[\mathcal{H}+eE_0x]^2}{2mc^2}\ , \quad \text{(C1)}$$

where $\mathcal{H}$ is the nonrelativistic operator Eq. (1) and $\mathcal{V}_0=-E_0x$. The energy eigenvalues of (C1) are given by first-order perturbation

$$\hat{\mathcal{E}}_{n,q}=mc^2+\mathcal{E}_{n,q}-\left\langle\phi_n\left|\frac{[\mathcal{H}+eE_0x]^2}{2mc^2}\right|\phi_n\right\rangle\ , \quad \text{(C2)}$$

where the classic contribution is given by (6)

$$\mathcal{E}_{n,q}=(n+\tfrac{1}{2})\hbar|\Omega|+\hbar qu-\tfrac{1}{2}mu^2\ . \quad \text{(C3)}$$

The perturbative correction is written as

$$\frac{[\mathcal{H}+eE_0x]^2}{2mc^2}=\frac{1}{2mc^2}\left[\mathcal{H}_2+2eE_0x\mathcal{H}+e^2E_0^2x^2-i\hbar\frac{2eE_0}{2m}P_x\right]\ , \quad \text{(C4)}$$

where use was made of the commutation relation $P_xx-xP_x=-i\hbar$ in the computation of $(eE_0/2m)[P_x^2x+xP_x^2]=(eE_0/2m)[2xP_x^2-2i\hbar P_x]$. Using (C4) inside (C2) yields

$$\hat{\mathcal{E}}_{n,q}=mc^2+\mathcal{E}_{n,q}+\frac{1}{2mc^2}\left\{\mathcal{E}_{n,q}^2+2eE_0\mathcal{E}_{n,q}\langle\phi_n|x|\phi_n\rangle+e^2E_0^2\langle\phi_n|x^2|\phi_n\rangle-i\hbar\frac{eE_0}{m}\langle\phi_n|P_x|\phi_n\rangle\right\}$$
$$=mc^2+\mathcal{E}_{n,q}+\frac{1}{2mc^2}\left\{\mathcal{E}_{n,q}^2+e^2E_0^2\frac{\hbar}{2m\Omega}(2n+1)\right\}\ , \quad \text{(C5)}$$

where use was made of $\langle\phi_n|x|\phi_n\rangle=\langle\phi_n|P_x|\phi_n\rangle=0$. Expanding $\mathcal{E}_{n,q}^2$ from (C3) and rearranging terms

$$\hat{\mathcal{E}}_{n,q}=mc^2+\hbar qu-\tfrac{1}{2}mu^2+(n+\tfrac{1}{2})\hbar|\Omega|\left[1-(n+\tfrac{1}{2})\frac{\hbar|\Omega|}{2mc^2}+\frac{\hbar qu}{mc^2}\right]+\frac{(\hbar qu-mu^2/2)^2}{2mc^2}\ . \quad \text{(C6)}$$

Retaining relativistic corrections in the cyclotron oscillation energy n, neglecting terms proportional to u^2/c^2 in the slow-wave region $u/c\ll1$, and subtracting mc^2 yields Eq. (49).

[1] O. Buneman, in *Crossed Field Microwave Devices,* edited by E. Okress (Academic, New York, 1961), p. 367.
[2] J. Feinstein, in *Crossed Field Microwave Devices* (Ref. [1]), p. 554.
[3] G. Mourier, in *Crossed Field Microwave Devices* (Ref. [1]), p. 395.
[4] J. Schneider, Phys. Rev. Lett. **12**, 504 (1959); J. L. Hirshfield and J. M. Wachtel, *ibid.* **19**, 533 (1964).
[5] H. Motz, J. Appl. Phys. **22**, 527 (1951); J. M. J. Madey, *ibid.* **42**, 1906 (1971).
[6] That is a consequence of the zero "rest mass" of a photon. An electron moving inside a slow-wave cavity or inside a plasma can emit a radiation quantum with no external fields present, because of the finite rest mass $\hbar\omega_{co}/c^2$ for a caviton and $\hbar\omega_p/c^2$ for a plasmon (ω_{co} and ω_p are the cutoff and plasma frequency).
[7] J. F. Hall, in *Crossed Field Microwave Devices* (Ref. [1]), p. 496.
[8] R. W. Gould, J. Appl. Phys. **28**, 599 (1957).
[9] S. Riyopoulos, IEEE, Trans. Plasma Sci. **22**, 626 (1994).
[10] J. Browning, C. Chan, J. Z. Ya, and T. E. Ruden, IEEE Trans. Plasma Sci. **19**, 598 (1991).
[11] A. Friedman, A. Gover, G. Kurizki, S. Ruschin, and A. Yariv, Rev. Mod. Phys. **60**, 471 (1988).
[12] S. Riyopoulos (unpublished).
[13] S. Riyopoulos, Phys. Plasmas, **2**, 935 (1995).